Hindawi
Journal of Food Processing and Preservation
Volume 2023, Article ID 2230456, 16 pages
https://doi.org/10.1155/2023/2230456

Research Article

Anti-skin Aging Potential of *Sargassum thunbergii* Ethanolic Extract: Antioxidant, Anti-inflammatory, and Antiwrinkle Effects on L929 Fibroblast Cells

Lulu Cui,[1] Haidong Qu,[2] Kun Qiao,[3] Shuji Liu,[3] Jingna Wu,[4] Yongchang Su,[3] Bei Chen,[3] and Zhiyu Liu[3]

[1]*College of Food Sciences and Technology, Shanghai Ocean University, Shanghai 200090, China*
[2]*College of the Environment and Ecology, Xiamen University, Xiamen, Fujian 361102, China*
[3]*Fisheries Research Institute of Fujian, Key Laboratory of Cultivation and High-Value Utilization of Marine Organisms in Fujian Province, Xiamen, Fujian 361013, China*
[4]*Xiamen Medical College, Xiamen, Fujian 361023, China*

Correspondence should be addressed to Bei Chen; chenbeifjfri@foxmail.com and Zhiyu Liu; 13906008638@163.com

Received 5 December 2022; Revised 2 July 2023; Accepted 9 August 2023; Published 6 September 2023

Academic Editor: Fabiano A.N. Fernandes

Increasing life expectancy of the human population has created a demand for functional food with anti-skin aging properties. Skin aging is a degenerative process caused by oxidative stress, inflammation, and matrix destruction. Some secondary metabolites isolated from marine macroalgae have been shown to exhibit potential dermatological benefits. The present study investigated the skin-protective properties of the ethanolic extract from *Sargassum thunbergii* (STEE) via antioxidant, anti-inflammatory, and antiwrinkle effects on mouse fibroblast L929 cells. The optimal extraction conditions for STEE were determined as follows: ratio of liquid to solid 25 : 1 mL/g, concentration of ethanol 40.2%, and extraction time 40 min. STEE was further purified by adsorption using a macroporous resin, SP700. STEE exhibited high DPPH radical and hydroxyl scavenging activity *in vitro*, enhanced the viability of H_2O_2-treated L929 cells, and reduced intracellular ROS generation in a dose-dependent manner. Superoxide dismutase and glutathione peroxidase activities and total antioxidant capacity in H_2O_2-treated L929 cells were increased while malondialdehyde content was markedly reduced by pretreatment with STEE. The inhibitory effect of STEE on H_2O_2-induced inflammation was shown by the downregulation of tumor necrosis factor-α, interleukin-6, cyclooxygenase-2, and inducible nitric oxide synthase. Furthermore, STEE reduced the matrix metalloproteinase-2 expression and inhibited collagenase and elastase activities. Moreover, STEE was nonirritating to human skin at 100 mg/mL according to the *in vitro* skin irritation test using EpiSkin™. Hemolysis assay showed that the hemolysis EC50 (1275 μg/mL) of STEE is much higher than the maximum effective concentration (125 μg/mL) against H_2O_2 exposure. Our results demonstrate that STEE may be a good candidate for the development of anti-skin aging functional food and cosmetic products.

1. Introduction

As the average life expectancy of humans has been increasing, skin aging is gaining attention, and consequently, the skin aging-related nutraceutical market has been established as one of the largest markets in modern times. Skin aging is a consequence of the natural aging process and the presence of excessive amounts of reactive oxygen species (ROS) in skin exposed to xenobiotics or solar ultraviolet (UV) radiation. ROS are continuously generated during normal metabolism in skin cells and are rapidly removed by nonenzymatic and enzymatic antioxidants; however, uncontrolled release of ROS is implicated in numerous human skin disorders. ROS induce a number of transcription factors such as activator protein- (AP-) 1 and nuclear factor- (NF-) κB [1], thereby contributing to proinflammatory signaling cascades and the activation of inflammation-related factors including interleukin- (IL-) 6, tumor necrosis factor- (TNF-) α,

inducible nitric oxide synthase (iNOS), and cyclooxygenase-(COX-) 2 [2]. Enzymes such as hyaluronidase, collagenase, elastase, and matrix metalloproteinases (MMPs) play important roles in the degradation of the extracellular matrix (ECM), which is closely associated with skin aging and wrinkling. To counteract the aging process, the nutraceutical industry is focused on identifying compounds with antioxidant, anti-inflammatory, and MMP/elastase/collagenase inhibitory activities or compounds that can enhance collagen expression [3].

A number of secondary metabolites isolated from marine macroalgae have exhibited potential dermatological benefits. Phenolic compounds have emerged as one of the most extensively researched classes of active substances present in algae. For example, phenolic-enriched extracts of algae may show tyrosinase [4], hyaluronidase [5], and MMP [6] inhibitory activities, as well as antioxidant, anti-inflammatory [7], and antiallergenic [8] effects. Consequently, these extracts are desirable ingredients for use in functional foods and cosmetic products. The extraction of marine algae phenolic compounds is most commonly achieved by solvent extraction. In these extraction procedures, polar solvents such as methanol, ethanol, and acetone or their aqueous mixtures are used to obtain polar phenolic compounds such as phlorotannins [9]. Extracts destined for the food, pharmaceutical, and cosmetic industries are standardly prepared by an ethanol-based process [10].

Marine algae phenolic compounds may be purified by a number of techniques, such as chromatography [11], ultrafiltration [12], and liquid-liquid fractionation with ethyl acetate. However, the application of these processes for purification of phenolics for human consumption is limited. The main drawbacks of these methods include low yields, high costs, and the use of non-food-grade solvents. The macroporous resin separation method overcomes the majority of the limitations of these techniques and is approved by the Food and Drug Administration for food product purification [13]. Polyphenols are adsorbed on the resin via hydrophobic binding and aromatic stacking, and they are subsequently desorbed with a mixture of water and organic solvent (e.g., ethanol). Macroporous resins including HP-20 [14], XAD-16N [13], and HPD-300 [15] have been used for purification of marine algae polyphenols in the previous studies.

Sargassum thunbergii is a common brown algae species that is distributed along the marine coast of China and has great economic and ecological value for sea cucumber culturing and seaweed beds. *S. thunbergii* extracts have been reported to exhibit various beneficial health effects. For example, enzymatic-digested sulfated polysaccharide from *S. thunbergii* had protective effect against H_2O_2-induced oxidative stress in cells and zebrafish model [16]. Methanol-extracted polyunsaturated fatty acid components and indole derivatives of *S. thunbergii* attenuated ROS-mediated oxidative stress in cellular systems [17] and inhibited lipid accumulation and adipogenesis [18]. The genus *Sargassum* is known to produce interesting phenolic compounds of high molecular weight [19]. However, there are no reports on the anti-skin aging effects of the phenolic-enriched ethanol extract from *S. thunbergii*. Fibroblasts are a major cell component of the dermis and produce ECM proteins as well as structural proteins (collagen and elastin), adhesive proteins (laminins and fibronectin), glycosaminoglycans, and proteoglycans. L929 mouse fibroblasts are widely used as an *in vitro* system for skin toxicity assessment or skin exposure experiments [20]. In this study, we optimized the extraction process of ethanol extract to maximize the extraction efficiency of phenolic compounds from *S. thunbergii*; the resulting crude ethanol extract was enriched by application of the macroporous adsorption resin SP700. Furthermore, the anti-skin aging potential of the ethanolic extract from *S. thunbergii* (STEE) was evaluated using L929 cells.

2. Material and Methods

2.1. Materials and Preparation Procedure of S. thunbergii Extract. *S. thunbergii* was collected from Dongtou Islands, located in the southeast of Zhejiang Province in China, and its geographical location are 120° 59′ 45″-121° 15′ 58″ east longitude and 27° 41′ 19″-28° 01′ 10″ north latitude. It dried under the shade before storage at −20°C until use. *S. thunbergii* extract was prepared according to the method described by Kim et al. [14]. Samples were powdered using a grinder and extracted with 40% ethanol. The ethanolic extract was centrifuged and concentrated using a vacuum rotary evaporator (BUCHI, Switzerland). The concentrated solution was purified with macroporous adsorption resin (Mitsubishi Chemical Corporation, Japan) by adsorption-desorption. The purified solution was freeze-dried and stored at −20°C.

2.2. Response Surface Methodology (RSM). Optimization of extraction was performed using RSM. Based on preliminary single-factor screening (data not shown), solid/lipid ratio (X_1), ethanol concentration (X_2), and extraction time (X_3) were considered to be the most important variables affecting the STEE extraction process. The independent variables and their code variable levels are shown in Table 1.

Design-Expert (v8.0.6) software was used to develop the statistical design, RSM modeling, and data analysis. To verify the interactions between the major operating variables and to determine their effect on the extraction rate, we optimized the experimental protocols using the Box-Behnken statistical design method. According to this, as shown in Table 2, 17 experimental runs were required to investigate three parameters at three levels. This experimental design generates a second-degree polynomial model (Y) of the following form:

$$Y = aX_1 + bX_2 + cX_3 + dX_1^2 + eX_1X_2 + fX_1X_3 + gX_2^2 + hX_2X_3 + iX_3^2 + 1, \quad (1)$$

where Y represents the response variable, which in our case is the extraction rate; X_1, X_2, and X_3 are the levels of the independent variables; a, b, and c are the linear terms; e, f, and h are the interaction terms; d, g, and i are the quadratic terms; and l is a constant.

Table 1: Factors and level of response surface analysis.

Coding levels	Factors		
	Ratio of solid to liquid (X_1)	Ethanol concentration (X_2)	Extraction time (X_3)
-1	1 : 15	20	20
0	1 : 20	40	30
1	1 : 25	60	40

Table 2: The Box-Behnken design matrix for the coded variables.

Experiment run	Standard order	Ratio of solid to liquid (g/mL)	Ethanol concentration (%)	Extraction time (min)	Extraction rate (%)
1	15	20	40	30	1.61
2	5	15	40	20	1.40
3	11	20	30	40	1.50
4	4	25	50	30	1.53
5	1	15	30	30	1.29
6	7	15	40	40	1.54
7	9	20	30	20	1.35
8	8	25	40	40	1.71
9	13	20	40	30	1.61
10	3	15	50	30	1.44
11	14	20	40	30	1.57
12	2	25	30	30	1.48
13	6	25	40	20	1.49
14	16	20	40	30	1.60
15	12	20	50	40	1.52
16	10	20	50	20	1.38
17	17	20	40	30	1.58

The extraction rate (response of an experiment) is determined by the total polyphenol content of the sample using the Folin-Ciocalteu method.

2.3. Determination of Total Phenolic Content (TPC). The total phenolic content of the extracts was evaluated using the modified Folin-Ciocalteu reagent method [21]. Gallic acid was used as a standard phenolic compound at concentrations of 10, 20, 30, 40, and 50 μg/mL, respectively. 1 mL of extract solution containing 1 mg of extract in distilled water was added to 5 mL of the Folin-Ciocalteu reagent (10%) and mixed thoroughly. After 3-8 min, 4 mL of 7.5% Na_2CO_3 was added, and the mixture was allowed to stand for 1 h with occasional shaking. The resulting absorbance was measured at 765 nm using a microplate reader (Tecan, Morrisville, NC, USA).

2.4. Purification of STEE by Macroporous Adsorption Resin. Crude extracts were further purified by SP700 resin according to the method developed by the Liu Zhiyu Laboratory. Briefly, crude extracts were centrifuged at 12000 g for 30 min, and the supernatants were filtered using 0.45 μM filters. Prior to loading the extract, the chromatographic column (ND8/DB08 Ø: 10 mm; h: 300 mm) with SP700 resin (Mitsubishi Chemical, Japan) was equilibrated with 3 bed volumes (BV) of deionized water. Thereafter, the crude extracts (4 mg/mL) were loaded onto the resin at a flow rate of 1 BV/h. Following sample adsorption, the loaded resin was washed with 1 BV of deionized water. To desorb the STEE, the loaded SP700 macroporous resin was eluted with 40% (v/v) ethanol solution at a rate of 2 BV/h. The eluent was concentrated with a rotary evaporator (BUCHI, Switzerland) to remove ethanol. Ultimately, the purified concentrates of STEE were freeze-dried under vacuum and stored at -80°C.

2.5. Measurement of Antioxidant Activity In Vitro

2.5.1. DPPH Radical Scavenging Assay. The DPPH radical scavenging activity of STEE was determined by the modified previous method [22, 23]. L-Ascorbic acid was used as a positive control with antioxidant activity. In brief, STEE at various concentrations of 1.25, 2.5, 5, 10, 20, 40, and 80 μg/mL was mixed with ethanol solution of DPPH radical (final concentration was 150 μM) in equal amounts. L-Ascorbic acid is at the same concentration as STEE. After incubating this mixture for 30 min, the absorbance was measured at 517 nm using a spectrophotometer (Tecan, Morrisville, NC, USA).

2.5.2. Hydroxyl Radical Scavenging Assay. Hydroxyl radical scavenging activity was performed according to the

manufacturer's instructions (Jiancheng Bioengineering Institute, Nanjing, China). L-Ascorbic acid was used as a positive control with antioxidant activity. The concentrations of STEE and L-ascorbic acid were 12.5, 25, 50, 100, 200, 400, and 800 μg/mL, respectively.

2.5.3. Superoxide Anion Radical Scavenging Assay. Superoxide anion radical scavenging activity were performed according to the manufacturer's instructions (Jiancheng Bioengineering Institute, Nanjing, China). L-Ascorbic acid was used as a positive control with antioxidant activity. The concentrations of STEE and L-ascorbic acid were 0.3125, 0.625, 1.25, 2.5, 5, 10, and 20 mg/mL, respectively.

2.6. Cell Culture. L929 murine fibroblast cell line was supplied by Prof. Yutian Pan (the Engineering Technological Center of Mushroom Industry, Minnan Normal University, China). The cells were cultured in RPMI1640 medium (Life Technologies, Carlsbad, CA, USA) supplemented with 10% fetal bovine serum (FBS), 100 mg/mL penicillin, and 100 U/mL streptomycin at 37°C and 5% CO_2.

2.7. Cell Viability Assay. Cell viability was evaluated with 3-(4,5-dimethylthiazol-2-yl)-5-(3-carboxymethoxyphenyl)-2-(4-sulfophenyl)-2H-tetrazolium (MTS) using the CellTiter 96 AQueous Non-Radioactive Cell Proliferation assay (Promega, Madison, WI, USA) according to the manufacturer's instructions. Briefly, L929 cells were seeded in 96-well plates at 10^4 cells/well and allowed to attach overnight. After serum starvation by culturing in medium containing 3% FBS for 12 h, the cells were treated with different concentrations of STEE (0-1000 μM) or H_2O_2 (0-500 μM) for 24 h and 3 h, respectively. After adding 20 μL MTS solution for another 45 min, the absorbance at 490 nm was measured with a microplate reader (Tecan, Morrisville, NC, USA). At least three independent experiments were performed.

2.8. Cellular Antioxidant Enzyme Activity and Lipid Peroxidation. Cellular antioxidant enzyme activity and intracellular lipid peroxidation were evaluated according to the method described by Chen et al. [22, 23]. Briefly, L929 cells were cultured in 60 mm tissue culture dishes at 7×10^5 cells/dish. After treatment with different concentrations of STEE (0, 31.25, 62.5, and 125 μg/mL) and 200 μM H_2O_2 for 24 h and 6 h, respectively, the cells were collected and resuspended in 400 μL phosphate-buffered saline (PBS). The cells were disrupted using TissueLyser II (Qiagen, Hilden, Germany), and superoxide dismutase (SOD) and glutathione peroxidase (GSH-Px) activities, as well as total antioxidant capacity (T-AOC) of the lysates, were measured with appropriate assay kits (Jiancheng Bioengineering Institute, Nanjing, China) according to the manufacturer's instructions. Intracellular lipid peroxidation was evaluated by measuring malondialdehyde (MDA) production using the manufacturer's instructions in commercial kit (Jiancheng Bioengineering Institute, Nanjing, China).

2.9. Measurement of Intracellular ROS Production. The free radical scavenging activity of STEE was evaluated using 1,1-diphenyl-2-picryl-hydrazyl. Briefly, L929 cells were seeded in a 24-well microplate at 1×10^5 cells/well. After 12 h of serum starvation and 24 h of STEE treatment, 25 μM 2′,7′-dichlorodihydrofluorescein diacetate (DCFH-DA) prepared in phenol red-free RPMI1640 medium was added to the cells for 30 min at 37°C in the dark. After two washes with prewarmed PBS, 200 μM H_2O_2 prepared in phenol red-free RPMI1640 with 10% FBS was added for 30–45 min at 37°C in the dark. The cells were washed and maintained in phenol red-free RPMI1640 containing 10% FBS for fluorescence microscopy observation (excitation/emission: 485/535 nm). For flow cytometry analysis, cells were treated with trypsin (without EDTA) for 4 min at 37°C until most of the cells were detached. The cells were centrifuged and washed twice with PBS, resuspended in phenol red-free RPMI1640 medium containing 10% FBS, and then measured using a flow cytometer within 1 h.

2.10. RNA Isolation, Reverse Transcription, and Quantitative PCR (qPCR) Analysis. L929 cells were pretreated with different concentrations of STEE for 24 h. This study was evaluated according to the method described by Chen et al. [22, 23]. Briefly, the total RNA sample was collected and extracted using an RNAprep Pure kit (Tiangen Biotech, Beijing, China) at 1 h and 3 h after the end of exposure to 200 μM H_2O_2. Reverse transcription was performed with 1 μg total RNA using a PrimeScript RT Master Mix (Takara Bio, Otsu, Japan), and real-time qPCR was performed using a FastStart Universal SYBR Green Master kit. The primers used for amplification of the target genes (inflammation-related genes, such as COX-2, iNOS, TNF-α, and IL-6) and reference gene (glyceraldehyde 3-phosphate dehydrogenase, GAPDH) are listed in Table 3. Relative quantification of target gene expression levels was performed with the $2^{-\Delta\Delta Ct}$ method [24].

2.11. Evaluation of MMP Inhibitory Activity by Gelatin Zymography. MMP-2 and MMP-9 activities in L929 cells treated with STEE were assessed by gelatin zymography. Cells were seeded in 6-well plates and cultured overnight and then treated with STEE in serum-free medium for 24 h. Conditioned medium was collected and centrifuged to remove dead cells, and the total protein content of 10x concentrated conditioned medium was determined with the Bradford assay [27]. The concentrated medium was resolved on a 10% polyacrylamide gel containing 1% gelatin. After electrophoresis, the gel was washed twice with 50 mM Tris-HCl (pH 7.5) containing 2.5% Triton X-100 at room temperature to remove SDS, rinsed, and incubated at 37°C in buffer containing 5 mM $CaCl_2$, 1 μM $ZnCl_2$, 50 mM Tris-HCl, and 1% Triton X-100 for 24 h to allow the digestion of gelatin by MMP. The gel was stained with Coomassie blue R250 staining solution for 30 min. Areas of gelatin hydrolyzed by MMP were visualized as white bands by a three-step destaining.

2.12. Evaluation of Elastase/Collagenase Inhibitory Activity. The inhibition of elastase and collagenase activities by STEE was evaluated as previously described [28]. The assay for elastase inhibition was performed in HEPES buffer (0.1 M

Table 3: Primers used for qPCR.

Gene	Primer sequence (5′→3′)	GenBank accession no. or reference
GAPDH	TCATTGACCTCAACTACAGGT CTAAGCAGTTGGTGGTGCAG	[25]
IL-6	CCCAATTTCCAATGCTCTCC TCCACAAACTGATATGCTTAGG	[26]
COX-2	TGCACTATGGTTACAAAAGCTGG TCAGGAAGCTCCTTATTTCCCTT	NM011198
NOS-2	GTTCTCAGCCCAACAATACAAGA GTGGACGGGTCGATGTCAC	NM010927
TNF-α	ACAAGGCTGCCCCGACTAC	[26]

HEPES with 0.5 M sodium chloride (pH 7.5)). Human leukocyte elastase (Sigma-Aldrich, St. Louis, MO, USA; E8140) was dissolved in sterile water to obtain a 1 μg/mL stock solution. The substrate N-(methoxysuccinyl)-Ala-Ala-Pro-Val-4-nitroanilide (MAAPVN) (Sigma-Aldrich; M4765) was dissolved in sterile water at 1 mM. A 25 μL volume of HEPES buffer, 25 μL elastase, and 25 μL of test extract were added to a 96-well plate. The blank contained 75 μL HEPES buffer, and the control contained 25 μL elastase and 50 μL HEPES buffer; (−)epigallocatechin-3-gallate (EGCG; 0.114 mg/mL) was used as a positive control. The plate was incubated at 25°C for 20 min. A 100 μL volume of MAAPVN was added to each well, and the plate was incubated for 40 min at 25°C. The optical density (OD) at 410 nm was measured on a microplate reader, and the inhibition rate was calculated as follows: $\text{inhibition rate}\,(\%) = [1 - (\text{OD}_{\text{sample}} - \text{OD}_{\text{blank}})/(\text{OD}_{\text{control}} - \text{OD}_{\text{blank}})] \times 100\%$.

The collagenase inhibition assay was performed in 50 mM tris(hydroxymethyl)-methyl-2-aminoethane sulfonate (TES) buffer (Sigma-Aldrich; T1375) with 0.36 mM $CaCl_2$ (pH 7.4). The collagenase substrate N-[3-(2-furyl)acryloyl]-Leu-Gly-Pro-Ala (FALGPA) (Sigma-Aldrich; F5135) was dissolved in sterile water to achieve a final concentration of 1 mM. Collagenase from *Clostridium histolyticum* (Sigma-Aldrich; C0130) was dissolved in TES buffer at a concentration of 1 mg/mL. Sodium citrate (200 mM (pH 5.0)) and ninhydrin solution (4%, *w*/*v*) were added to sterile water. Each experimental group consisted of 25 μL collagenase, 25 μL TES buffer, and 25 μL of the test sample. The blank groups contained 75 μL TES buffer, the negative control groups contained 25 μL collagenase and 50 μL TES buffer, and the positive control groups contained 25 μL collagenase, 25 μL TES buffer, and 25 μL EGCG (0.114 mg/mL). The tubes were incubated in a water bath at 37°C for 20 min. A 100 μL volume of FALGPA was added to each tube, followed by incubation for 60 min at 37°C. Equal volumes of sodium citrate and ninhydrin solution were combined, and 200 μL of the mixture was added to each tube; the tubes were placed in a boiling water bath for 5 min, and when they had cooled, 200 μL of 50% isopropanol was added. The content of each tube was transferred to a 96-well plate, and the absorbance at 540 nm was read on a microplate reader.

2.13. In Vitro Skin Irritation Test. The *in vitro* skin irritation test was conducted based on the test guidelines of the Organization for Economic Co-operation and Development (OECD TG439) [29] and standard operating procedures for the EpiSkin™ skin irritation test method. The epidermis units were transferred to wells of 12-well plates containing 2 mL maintenance media and preincubated in a 37°C, 5% CO_2 incubator for at 24 h. After preincubation, the epidermis units were exposed to 10 μL STEE (1, 10, 100 mg/mL), 5% SDS (positive control), or H_2O (negative control) for 15 min at room temperature. After the 15 min exposure, treated units were rinsed thoroughly with 25 mL of sterile PBS to remove all residual test material from the epidermal surface. The remaining PBS on the surface was wiped with cotton bud without damaging the epidermis. The tissue units were transferred into wells prefilled with the new maintenance medium and incubated at 37°C, 5% CO_2 for 42 h. The EpiSkin™ units were transferred to the MTT-filled wells (0.3 mg/mL) for 3 h at 37°C, 5% CO_2. The tissue units were removed with a punch, and the epidermis was gently separated from the collagen matrix; both parts were placed into the microtubes, and 500 μL of acidic isopropanol was added to each tube. The tubes were stored for 4 h at room temperature and protected from light. Each tube was vortexed at the middle of the incubation period to help extraction. Two wells per tissue were transferred from each tube into a 96-well plate, and the absorbance at 570 nm was read on a microplate reader.

2.14. Hemolysis Assay. The horse erythrocyte hemolysis experiment was carried out as previously described [30]. A 4% horse erythrocyte suspension was prepared in PBS solution. Different concentrations of STEE were incubated with an equal volume of horse erythrocytes at 37°C for 2 h. PBS and Triton X-100 were used as negative and positive controls, respectively. Centrifuge the solution at $900 \times g$ for 5 minutes, followed by the transfer of 200 μL of the resulting supernatant to a 96-well plate. Subsequently, the OD value of each well was measured at a wavelength of 500 nm.

2.15. Statistical Analysis. All assays were replicated three times, and the experimental results were expressed as means ± standard deviations. The statistical analysis was carried

Table 4: Analysis of variance of the experimental results.

Source	Sum of square	df	Mean square	F value	p value
Model	0.18	9	0.020	29.56	<0.0001
X_1	0.036	1	0.036	53.21	0.0002
X_2	7.813×10^{-3}	1	7.813×10^{-3}	11.41	0.0118
X_3	0.053	1	0.053	77.10	<0.0001
X_1X_2	2.500×10^{-3}	1	2.500×10^{-3}	3.65	0.0977
X_1X_3	1.600×10^{-3}	1	1.600×10^{-3}	2.34	0.1703
X_2X_3	2.500×10^{-3}	1	2.500×10^{-3}	0.036	0.8539
X_1^2	3.981×10^{-3}	1	3.981×10^{-3}	5.81	0.0467
X_2^2	0.069	1	0.069	101.10	<0.0001
X_3^2	3.36×10^{-3}	1	3.36×10^{-3}	4.91	0.0624
Residual	4.795×10^{-3}	7	6.850×10^{-4}	—	—
Lack of fit	3.475×10^{-3}	3	1.158×10^{-3}	3.51	0.1283
Pure error	1.420×10^{-3}	4	3.300×10^{-4}	—	—
Cor total	0.19	16	—	—	—

out by one-way analysis of variance (ANOVA) using GraphPad Prism. Prism reports results as nonsignificant (ns) at $p > 0.05$, significant (symbolized by "*") at $0.01 < p \leq 0.05$, very significant ("**") at $0.001 < p \leq 0.01$, and extremely significant ("***") at $p < 0.001$.

3. Results

3.1. Extraction Optimization

3.1.1. Model Fitting and Statistical Analysis. The design matrix and the corresponding results of the RSM experiments are presented in Table 2. By applying multiple regression analysis to the experimental data, a second-order polynomial equation, which describes the correlation between STEE extraction rate and the three variables, was obtained, as below:

$$\begin{aligned} Y(\%) = {} & 1.59 + 0.068X_1 + 0.031X_2 + 0.081X_3 - 0.025X_1X_2 \\ & + 0.02X_1X_3 - 0.0025X_2X_3 - 0.031X_1^2 \\ & - 0.13X_2^2 - 0.028X_3^2, \end{aligned}$$

$$R^2 = 0.9744, \quad (2)$$

where Y represents the STEE extraction rate and X_1, X_2, and X_3 represent the solid/lipid ratio, concentration of ethanol, and extraction time, respectively.

As shown in Table 4, the statistical significance of the model was determined by p value ($p < 0.0001$) and indicated that the model was highly significant. In addition, the F value (lack of fit) of 3.51 and the associated p value of 0.1283 indicated excellent correlation between the predicated and experimental values. The determination coefficient ($R^2 = 0.9744$) and the adjusted determination coefficient ($R^2_{adj} = 0.9414$) were used to test the applicability of the model, indicating a satisfactory correlation of rate values determined by experiment and those predicted by the equation. Furthermore, a low coefficient of variation (C.V.% = 1.74) clearly indicated high reliability of the experimental values. These results suggested that the model could work well for the prediction of polyphenol extraction rate from *S. thunbergii*.

3.1.2. Analysis of Response Surface Plot and Contour Plot. Response surfaces were plotted by Design-Expert software to assess the interactions between variables and to determine the optimal level of each independent variable required to obtain the maximum response. 3D response surfaces are shown in Figure 1. Figures 1(a) and 1(c) illustrate the interaction surfaces of the ratio of solid/liquid with ethanol concentration and extraction time, respectively. The steep slopes and elliptical contours observed in these figures indicate a substantial effect magnitude and strong interaction between the variables. Figure 1(b) displays the interaction surface between the ratio of solid/liquid and extraction time, revealing a flat surface. This observation suggests a weaker influence and a less significant interaction between these variables.

3.1.3. Verification of Predictive Model. To determine the accuracy of the model equation, a verification experiment was carried out based on the optimal conditions: ratio of liquid to solid, 25 : 1 mL/g; concentration of ethanol, 40.2%; and extraction time, 40 min. The mean extraction rate ($n = 3$) of polyphenol was 1.703%, which correlates closely with the predicted value of 1.704%. This demonstrates and verifies the accuracy of the response model and indicates that the model designed in the study is both fit for the purpose and accurate.

3.2. Characterization of STEE Desorbed Using SP700 Macroporous Resin. In the primary extract, that is, prior to static adsorption and desorption, the TPC of STEE was

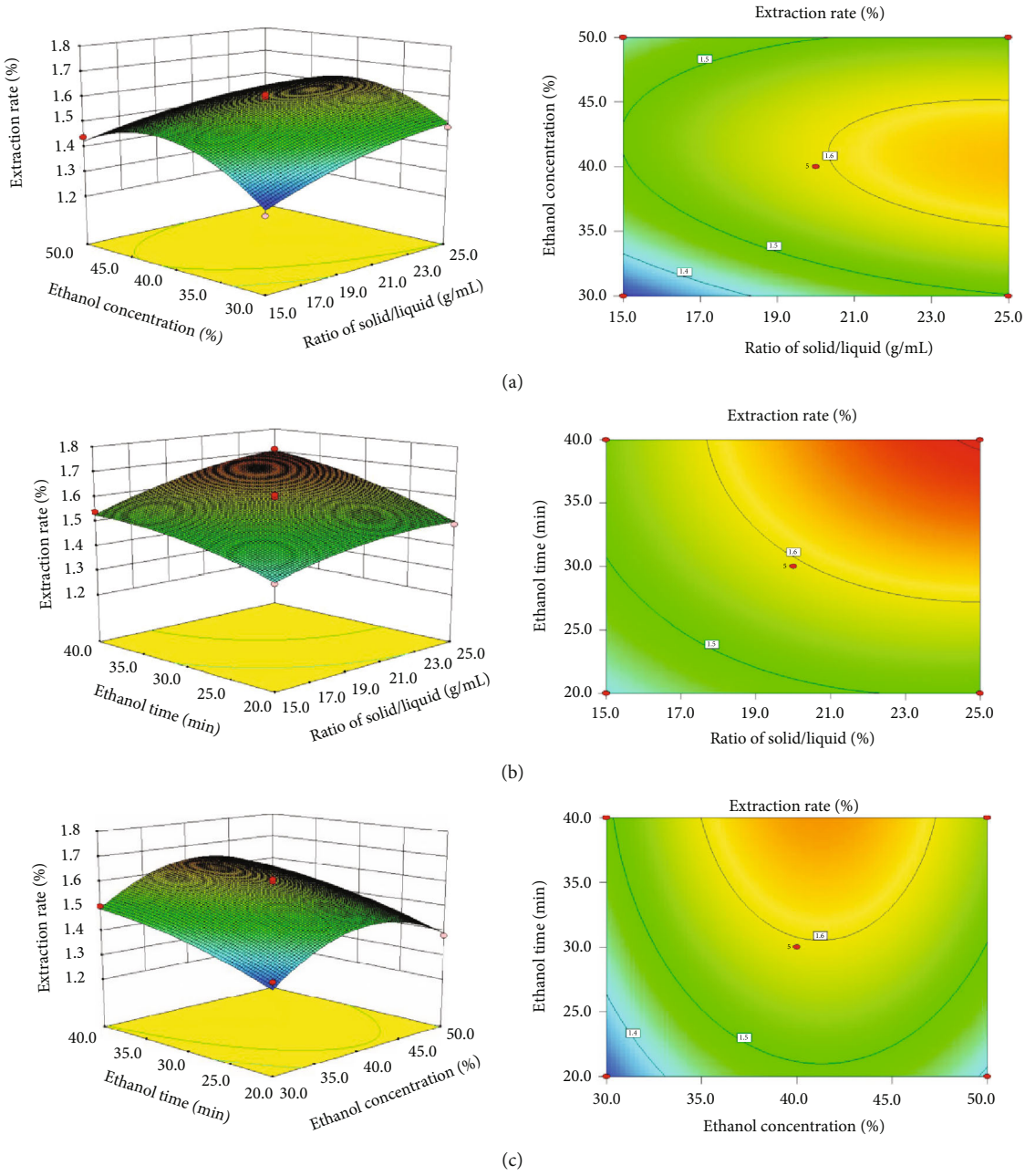

Figure 1: Response surface 3D plots and contour plots of the effect of various factor interactions on extraction rate of phlorotannins:(a) ratio of solid to liquid and ethanol concentration, (b) ratio of solid to liquid and extraction time, and (c) ethanol concentration and extraction time.

6.7%. The phenolic concentration of STEE desorbed from SP700 was 43.4%. Therefore, the use of SP700 facilitated enrichment (6.5 times) of polyphenol in the fraction desorbed with respect to the primary extract. DPPH, hydroxyl, and superoxide anion radical scavenging activities were used to determine *in vitro* antioxidant activity, and the results are shown in Figure 2. STEE and L-ascorbic acid exhibited significantly antioxidant activities to DPPH, hydroxyl, and superoxide anion radicals *in vitro*. The half maximal inhibitory concentration (IC_{50}) values of STEE and L-ascorbic acid to DPPH radical scavenging activities were 2.713 μg/mL and 6.237 μg/mL, respectively (Figure 2(a)). The IC_{50} values of STEE and L-ascorbic acid to hydroxyl radical scavenging activities were 81.32 μg/mL and 235.4 μg/mL, respectively (Figure 2(b)). The IC_{50} values of STEE and L-ascorbic acid to superoxide anion radical scavenging activities were 9.718 mg/mL and 0.2552 mg/mL, respectively (Figure 2(c)). STEE exhibited substantially higher DPPH radical and hydroxyl radical scavenging activities compared to L-ascorbic acid. However, the superoxide anion radical scavenging activity of STEE was considerably weaker than that of L-ascorbic acid.

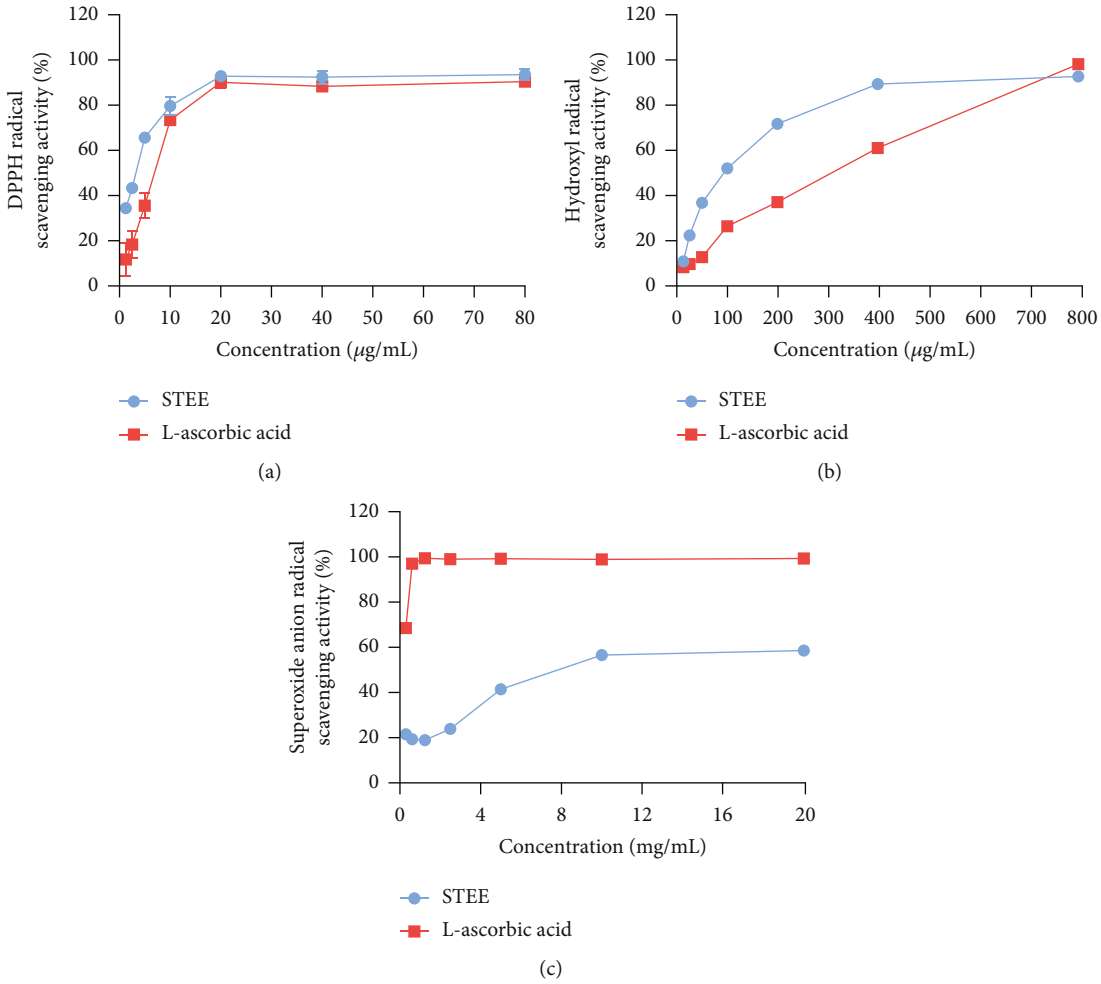

Figure 2: *In vitro* radical scavenging activity of STEE: (a) DPPH radical, (b) hydroxyl radicals, and (c) superoxide anion radical scavenging activity of STEE in comparison to L-ascorbic acid.

3.3. STEE Reversed the H_2O_2-Induced Decrease in Cell Viability. L929 cells were first treated with various concentrations of STEE (0–1000 μg/mL) for 24 h to determine whether STEE is cytotoxic. STEE at concentrations of 31.25–250 μg/mL had no effect on cell viability relative to the control group ($p > 0.05$; Figure 3(a)), although it was toxic at 500 μg/mL ($p < 0.05$). Therefore, 31.25–250 μg/mL STEE was used in subsequent assays.

Cells were treated with various concentrations of H_2O_2 (0-500 μM) for 3 h to determine the H_2O_2 concentration that would induce oxidative damage. H_2O_2 reduced cell viability in a concentration-dependent manner (Figure 3(b)); 200 μM H_2O_2 reduced viability by approximately 50% and was selected as the concentration used in subsequent experiments. Cell viability was reduced to 75.5% of the control value upon exposure to H_2O_2 (Figure 3(c)). However, pretreating the cells with STEE (31–125 μg/mL) reversed this effect in a concentration-dependent manner.

3.4. Intracellular ROS Scavenging Effects of STEE. DCFH-DA, a nonfluorescent compound, is hydrolyzed by intracellular esterase upon crossing the plasma membrane and entering the cytoplasm. This conversion yields nonfluorescent DCFH, which is subsequently oxidized to fluorescent DCF by intracellular ROS, resulting in green fluorescence. Therefore, the fluorescence intensity serves as an indicator of cellular ROS levels [31]. This study is aimed at investigating the effects of different concentrations of STEE (0-125 μg/mL) and H_2O_2 (200 μM) on intracellular ROS levels. The scavenging effect of STEE was assessed using fluorescence microscopy and flow cytometry. The fluorescence microscopy results demonstrated a notable elevation in green fluorescence following exposure to H_2O_2. However, the preincubation of STEE exhibited a marked reduction in the green fluorescence levels (Figure 4(a)). The flow cytometry analysis revealed a 9.4-fold increase in ROS levels in H_2O_2-exposed cells compared to control cells. Additionally, the gradual decrease in peak displacement (Figure 4(b)), representing the ROS level, was observed after the addition of STEE to the cells at 24 h.

3.5. STEE Enhanced Antioxidant Activity and Inhibited Lipid Peroxidation. SOD and GSH-Px are two important antioxidant enzymes that protect tissue from oxidative damage. We evaluated the protective mechanisms of STEE by measuring the levels of SOD, GSH-Px, and T-AOC. Compared

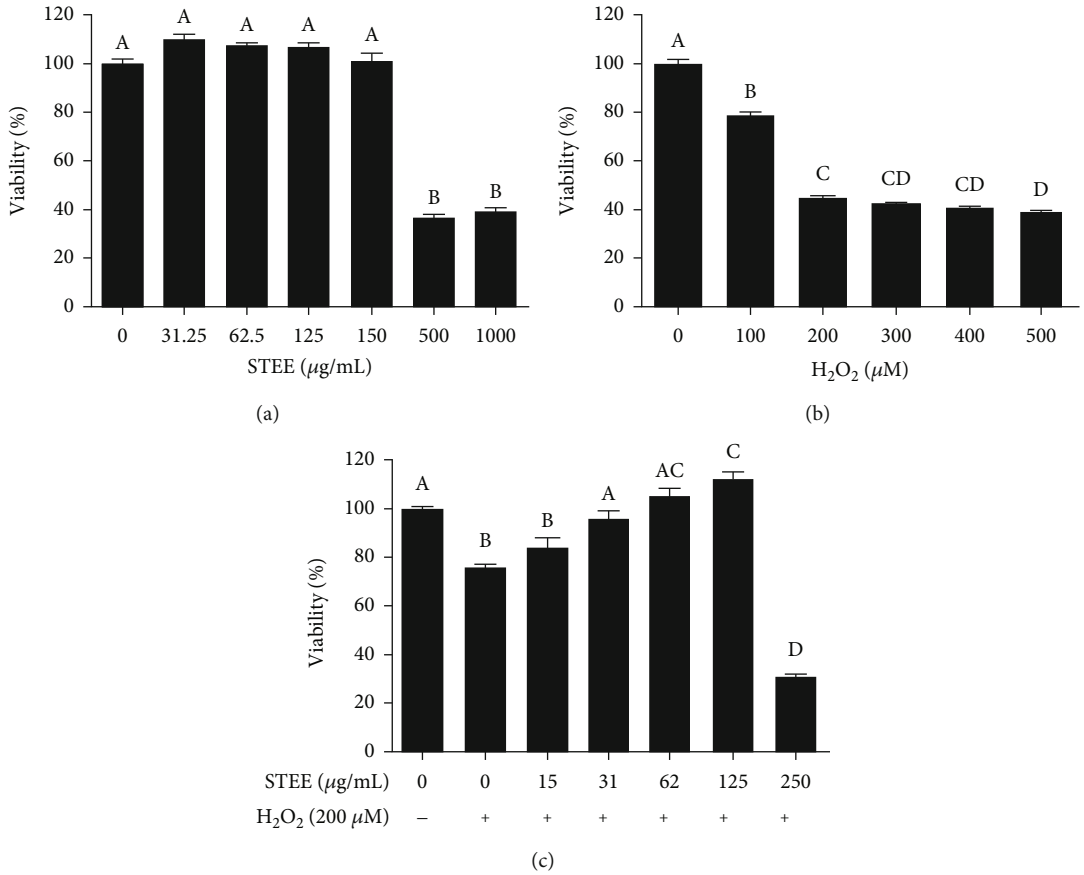

Figure 3: The effects of (a) STEE and (b) H_2O_2 at different concentrations on L929 cell viability and (c) the protective effects of STEE on L929 cells damaged by H_2O_2. The error bars refer to the standard deviations obtained from the triplicate sample analysis. The data were analyzed by one-way ANOVA followed by Tukey's *post hoc* test. The means of treatments not sharing a common letter (A-D) are significantly different (comparison between all the treatments) ($p < 0.05$).

to the control group, SOD, T-AOC, and GSH-Px were decreased by H_2O_2 exposure, but this was abrogated by STEE pretreatment. We also found that the increase in MDA content induced by H_2O_2 ($p < 0.05$)—reflecting the oxidation of cellular lipids due to oxidative stress—was reversed by pretreatment with 62.5 or 125 μg/mL STEE ($p < 0.05$) (Figure 5).

3.6. STEE Alleviated H_2O_2-Induced Inflammation in L929 Cells. H_2O_2 exposure for 1 or 3 h stimulated the mRNA expression of proinflammatory genes, including *COX-2*, *iNOS*, *TNF-α*, and *IL-6*, as compared to control cells (Figure 6); treatment with STEE decreased the levels of these transcripts in a dose-dependent manner.

3.7. STEE Suppressed MMP-2, Elastase, and Collagenase Activities. We evaluated whether STEE alters the gelatinolytic activities of the MMP-2 and MMP-9 secreted by L929 cells by gelatin zymography. In gelatin zymography experiments, the band intensity corresponds to the activity levels of MMP-2 and MMP-9. Our findings revealed that the exposure of L929 cells to STEE resulted in a dose-dependent weakening of MMP-2 bands, while the MMP-9 bands did not exhibit significant changes (Figure 7(a)). Thus, STEE concentrations ranging from 0 μg/mL to 125 μg/mL demonstrated a significant reduction in MMP-2 enzymatic activity, while leaving MMP-9 activity largely unaffected. STEE at concentrations from 10 μg/mL to 100 μg/mL showed significant ($p < 0.05$) increases in inhibitory activities against collagenase and elastase. EGCG, which was used as a standard reference material, showed potent inhibitory effects against collagenase and elastase (Figure 7(b)).

3.8. Toxicity Assessment of STEE. In the *in vitro* skin irritation test, EpiSkin™ cell viability was 13.6 ± 0.9% in the 5% SDS-treated group. However, the viabilities of the STEE-treated groups were 94.6 ± 5.6%, 96.8 ± 2.2%, or 83.3 ± 4.2 % with 1, 10, or 100 mg/mL STEE treatment, respectively (Figure 8(a)). Based on OECD TG439, all the STEE preparations were nonirritants to human skin because the cell viabilities were above 50% after 15 min exposure and 42 h incubation.

To evaluate the cytotoxicity of STEE, horse erythrocytes were treated with 0-4000 μg/mL STEE. The results showed that as the concentration of STEE increased, hemolysis of horse erythrocytes was induced. It caused less than 10% hemolysis at concentrations up to 500 μg/mL. The EC50 of hemolysis effect is 1275 μg/mL which was a higher concentration than the observed maximum effective concentration (125 μg/mL) against H_2O_2 exposure (Figure 8(b)).

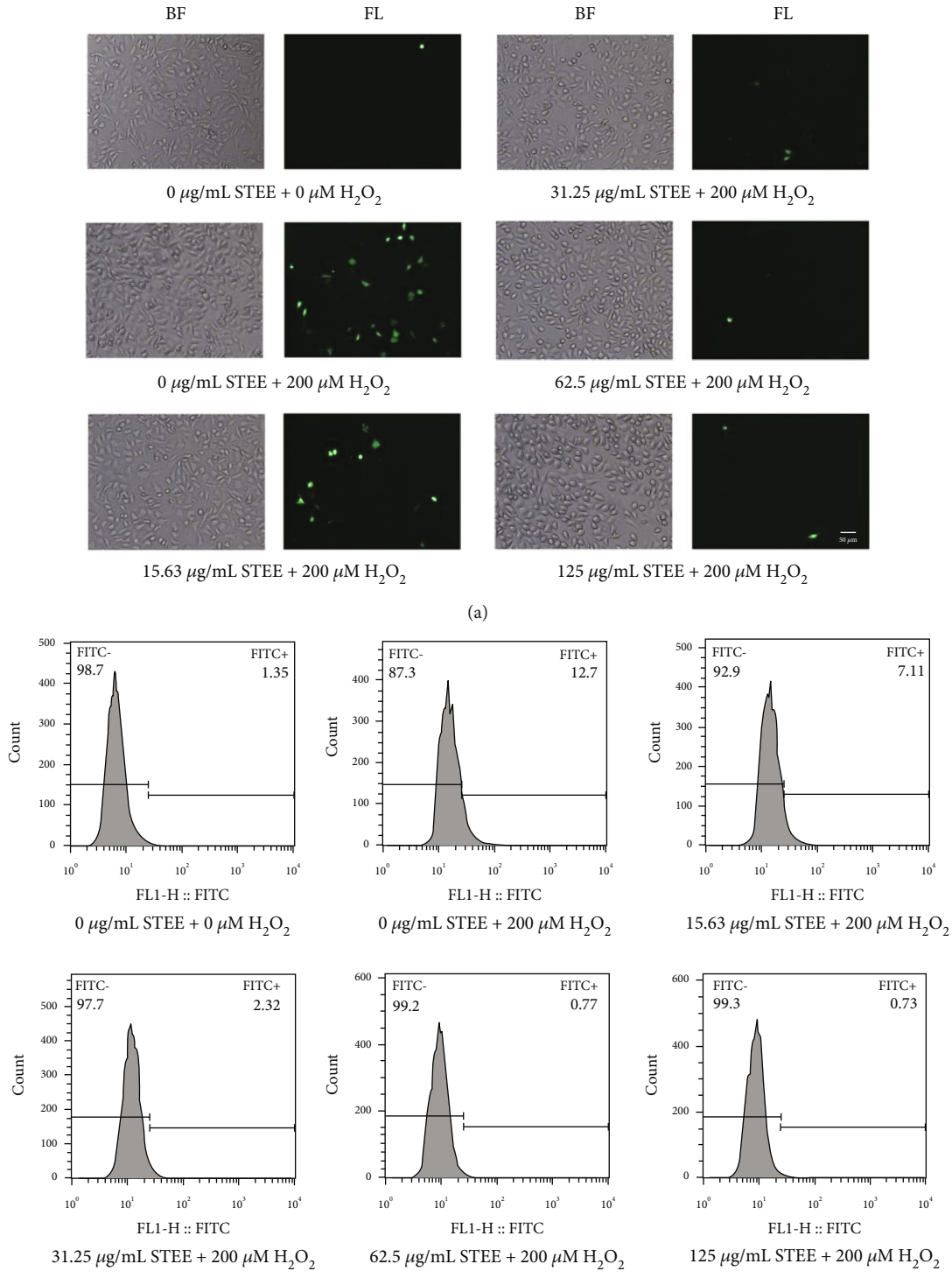

Figure 4: Effect of STEE on H_2O_2-induced ROS production in L929 cells, as analyzed by fluorescence microscopy (a) and flow cytometry (b). Cells were treated with different concentrations of STEE for 24 h and incubated in 200 μM H_2O_2 for 30-45 min. Control values were obtained in the absence of STEE and H_2O_2.

4. Discussion

Distinct Sargassum species have demonstrated efficacy in mitigating various dermal conditions including UVB photodamage, acne-induced inflammation, and hyperpigmentation [32, 33] as well as inflammation induced by fine particulate matter and compromised skin barrier functionality [34]. Phenolics are secondary metabolites that allow algae to adapt to environmental stressors such as UV radiation, heat, salinity, or cold. Hence, the extraction efficiency of

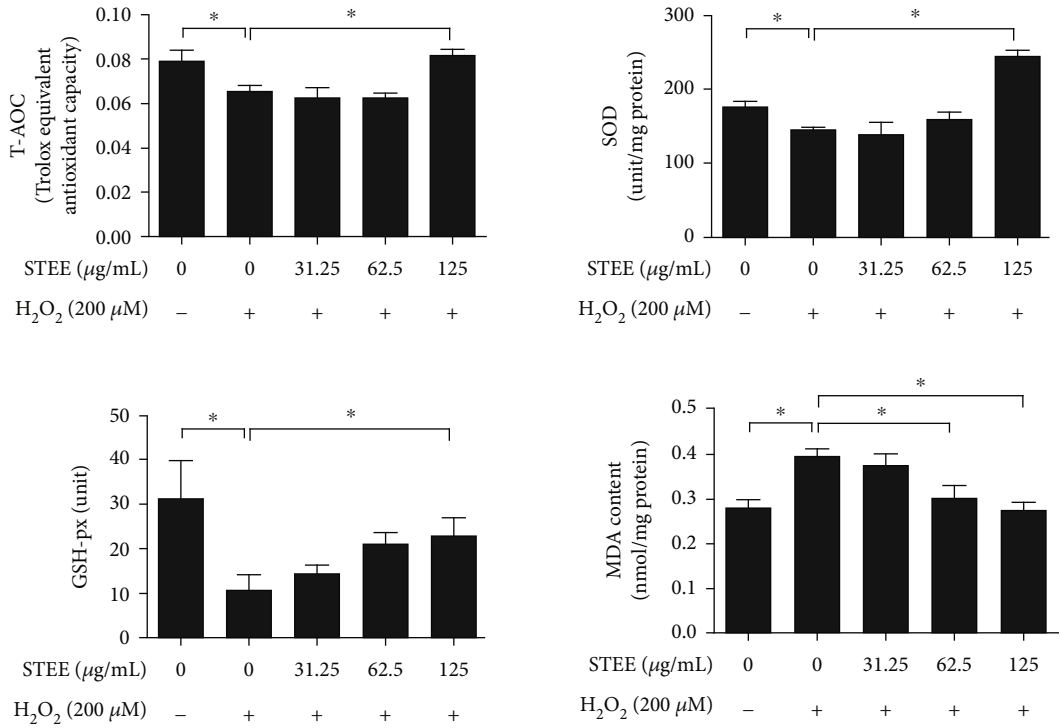

Figure 5: Effects of STEE on T-AOC, SOD, and GSH-Px activities as well as MDA content in L929 cells subjected to H_2O_2-induced oxidative stress. Means with "*" differ significantly ($p < 0.05$).

phenolic compounds serves as a crucial parameter in this study for obtaining the desired extracts. Aqueous ethanol is a safe and effective solvent and was our solvent choice for extraction of the polar phenolic compounds from brown algae. In the current study, we identified that 40% ethanol facilitated the optimal recovery of phenolic extracts from STEE. Otero et al. [35] reported higher recovery of phenolics in 50% ethanol than in pure ethanol. Gam et al. revealed that the free radical scavenging activity, tyrosinase inhibitory activity, and collagenase inhibitory activity of *S. thunbergii* extracts were optimized when the ethanol concentration was 53% [32]. In previous RSM studies, ethanol was identified as the single most important contributor in extraction of brown algae phenolics [36]. However, in this study, extraction time was identified as the most critical variable, that is, the variable that most affected the response process. The utilization of SP700 macroporous resin led to a remarkable 6.5-fold increase in the content of polyphenols in STEE. However, it remains the direction of our future research to continue to improve the purity of phenolic compounds and to clarify the structural characteristics of the major phenolic compounds that exert skin-protective effects in STEE.

Controlling radical levels seems to be a major mechanism through which we cope with skin aging. The present investigation delineates the potent antioxidant capabilities of *S. thunbergii* extract *in vitro*, as evidenced by its hydroxyl radical, DPPH radical, and intracellular ROS scavenging activities. Key players in cellular antioxidant defense such as superoxide dismutase (SOD), glutathione peroxidase (GSH-Px), and total antioxidant capacity (T-AOC) as well as malondialdehyde (MDA), a lipid peroxidation and cell injury indicator, were examined [37]. The escalation in SOD, T-AOC, and GSH-Px and the decrement in MDA level observed by STEE treatment indicated that STEE protects cells against oxidative damage by enhancing the antioxidant systems of fibroblasts. Extensive research has been conducted to employ a diverse array of extraction techniques for the extraction of bioactive natural antioxidants from *S. thunbergii*. In a study by Park et al., water-soluble extracts from *S. thunbergii* were prepared using carbohydrate hydrolysis which also showed efficient scavenging activity against hydroxyl, DPPH, and alkyl radicals [38]. The subcritical water extraction process yielded a highly effective extract of *S. thunbergii*, demonstrating notable scavenging activities against ABTS, DPPH, and FRAP radicals [39]. The methanolic extract of *S. thunbergii* significantly reduced intracellular ROS-mediated cell damage and upregulated the expression of SOD-1 and glutathione reductase at the mRNA and protein levels [17].

The link between ROS and skin inflammation is well known. The interaction between ROS and cytokines such as TNF-α and IL-6 leads to a vicious cycle that increases immune activation and oxidative damage and exacerbates skin inflammation. iNOS and COX-2 play an important role in immunity against infectious agents by stimulating the production of NO and prostaglandin E2, respectively [40], and were reportedly associated with 12-O-tetradecanoylphorbol-13-acetate- (TPA-) induced inflammation in mouse skin [41]. Additionally, the expression of both enzymes was enhanced in the skin of SKH-1 mice following benzanthrone and UVB exposure [42]. In the present study, COX-2, iNOS, TNF-α, and IL-6 levels were upregulated upon H_2O_2

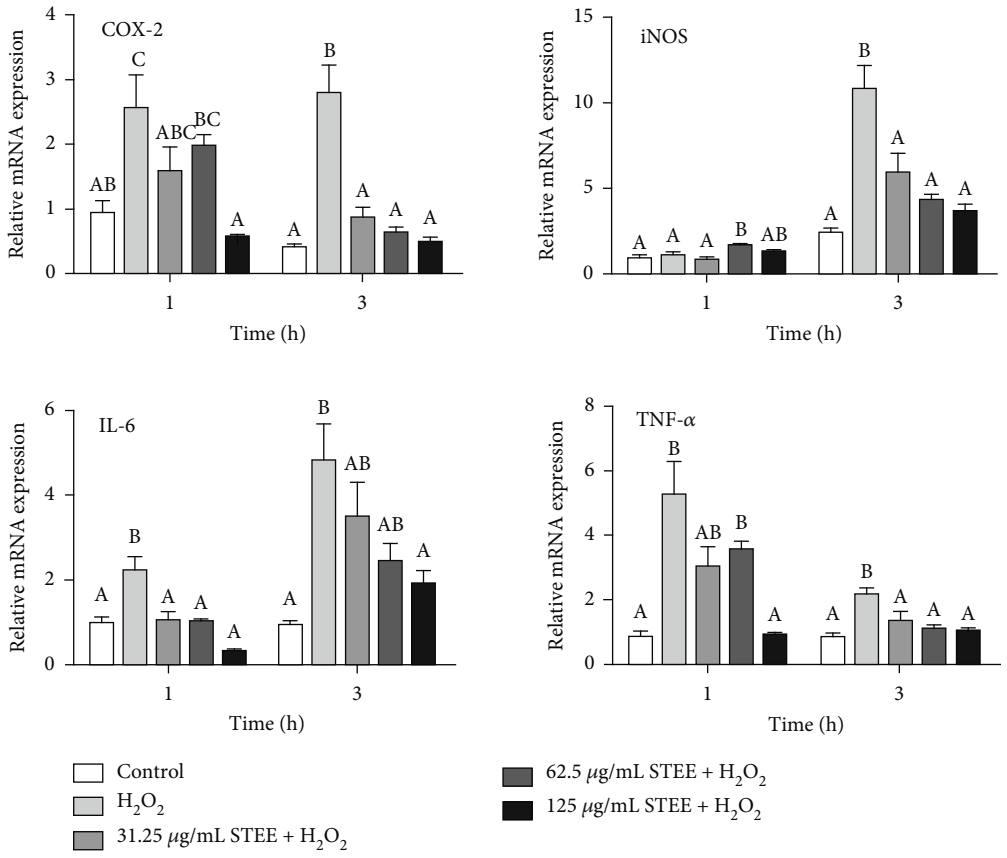

Figure 6: STEE inhibits H_2O_2-induced proinflammatory gene expression in L929 cells. Cells were pretreated with different concentrations of STEE (0, 31.25, 62.5, and 125 μg/mL) for 24 h. The mRNA expression of COX-2, iNOS, TNF-α, and IL-6 in L929 cells was measured by qPCR at 1 h and 3 h after the end of exposure to 200 μM H_2O_2. Bars represent means ± SEM of four samples per group. The data were analyzed by one-way ANOVA followed by Tukey's *post hoc* test. The means of treatments not sharing a common letter (A-C) are significantly different (comparison between treatments within each time point, $p < 0.05$).

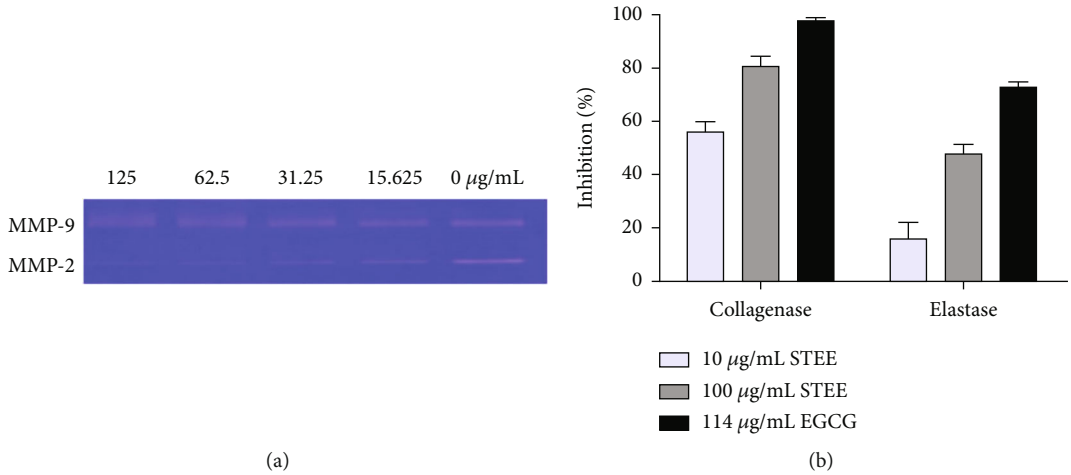

Figure 7: Antiwrinkle effects of STEE *in vitro*. The antiwrinkle effect of STEE was determined by gelatinolytic activities of MMP-2 and MMP-9 in L929 cells using gelatin zymography (a) and the inhibitory effects of STEE on collagenase and elastase (b). Means with different letters (A–C) differ significantly ($p < 0.05$).

exposure relative to the control group; however, this was reversed by pretreatment with STEE. This finding parallels that of our groups previous research, which demonstrated that the *S. thunbergii* polyphenol extract (STPE), purified using XDA-7 macroporous resin, exhibited a significant reduction in the expression of inflammatory factors in UVB-irradiated L929 cells. In addition, a multitude of studies have provided compelling evidence regarding the anti-

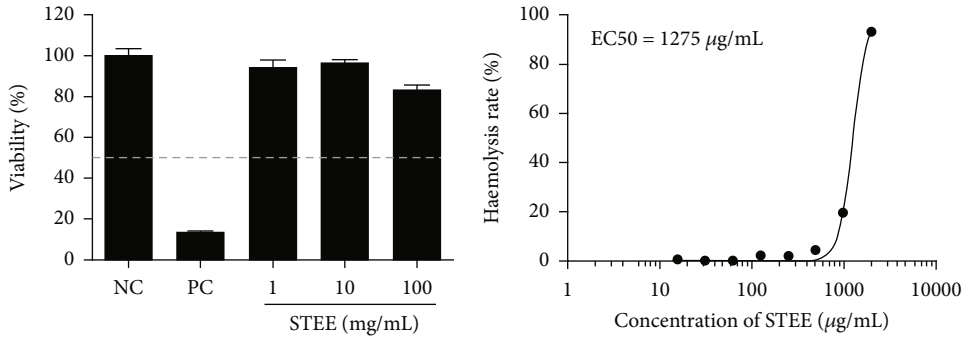

Figure 8: Toxicity assessment of STEE: (a) Cell viabilities of the 3D human skin model EpiSkin™ in the skin irritation test. An MTT assay was performed on EpiSkin™ samples treated with STEE for 15 min and postincubated for 42 h. NC and PC were treated with H_2O or 5% SDS, respectively; (b) the hemolytic activity of STEE on horse erythrocytes. The 100% hemolysis was conducted using the treatment of the positive control, 0.1% Triton X-100. The erythrocytes that was resuspended in PBS was used as negative control.

inflammatory effects of phenolic compounds extracted from diverse species of brown algae on skin cells. Dieckol from *E. cava* suppressed skin inflammation including atopic dermatitis in HaCaT human keratinocytes [7], and eckol from *Eisenia bicyclis* reduced the production of NO as well as iNOS, COX-2, and TNF-α expression in *Propionibacterium acnes*-induced HaCaT cells [43]. Phlorotannins extracted from brown seaweed *Ascophyllum nodosum* blocked lipopolysaccharide-induced TNF-α and IL-6 release by macrophages [44], and the anti-inflammatory effects of 6,6′-bieckol and 6,8′-bieckol were demonstrated in a mouse ear model induced by arachidonic acid, 12-O-tetradecanoylphorbol-13-acetate (TPA), and oxazolone [45].

Brown algae phenolics can potentially be used as an active ingredient in antiwrinkle cosmetic products owing to their MMP, hyaluronidase, collagenase, and elastase inhibitory activities [46]. In skin cosmetics, MMPs accelerate skin collagen and elastin fiber degradation. A total of 18 MMPs are expressed in the skin [47]. Collagen fibers are primarily degraded by MMP-1 and MMP-2, whereas elastin fibers are mainly degraded by elastases (i.e., MMP-2) and MMP-9 [48]. Gelatin zymography is used to evaluate the gelatin-degrading activities of proteolytic enzymes, such as MMP-2 (gelatinase A) and MMP-9 (gelatinase B) [49]. In this study, we found that STEE inhibited the gelatinolytic activity of MMP-2 in a dose-dependent manner without affecting L929 cell viability. Since the first report of the inhibitory effects of *E. cava* phlorotannins on MMP-2 and MMP-9 [50], 6,6′-bieckol from *E. cava* and eckol and dieckol from *Ecklonia stolonifera* have been shown to suppress MMP activity in human dermal fibroblasts [51, 52]. Our study indicated that MMP-9 activity was not reduced following treatment with STEE. The diversity and specificity of the MMP inhibitory property of natural products were proved in many studies. Qu et al. found that the level of MMP-2 mRNA expression and MMP-9 activity is significantly inhibited by a polysaccharide from *S. thunbergii*; however, there were no changes in MMP-9 mRNA expression and MMP-9 activity following the treatment [53]. In another study, the MMP inhibitory activities of caffeic acid and chlorogenic acid were investigated. The results indicated that caffeic acid inhibits MMP-1 and MMP-9, but not MMP-3, whereas chlorogenic acid inhibits MMP-3, but not MMP-1 and MMP-9 [54]. AE-941, an orally bioavailable standardized extract of cartilage, inhibits the gelatinolytic activity of MMP-2 and exerts minor inhibitory effects on MMP-1, MMP-7, MMP-9, and MMP-13 [55]. The catalytic domain of MMPs includes a notable S1′ "pocket" located to the right of the zinc atom. The depth, length, and amino acid sequence of the peptide around the S1′ pocket determine, to a large extent, the specificity of substrates and inhibitors [56]. The specificity of the MMP inhibitory property of STEE might be responsible for its structure and its binding modes with catalytic domains. Given that elastase and collagenase cause wrinkles and skin aging by degrading elastin and collagen, evaluating the antielastase and anticollagenase activities of STEE can provide useful information on its potential application as a cosmetic agent [57]. STEE was found to suppress the activities of human leukocyte elastase and *C. histolyticum* collagenase type 1; similar inhibition has also been shown for dieckol from *E. cava* [58] and *S. plagyophyllum* ethanol extract [59].

Tests of skin corrosion and irritation have long been performed using rabbits. However, the growing ethical recognition of animal welfare has prompted the replacement of *in vivo* testing of skin corrosion and irritation using animals by alternative methods using human skin models which closely mimics the biochemical and physiological properties of the upper parts of the human skin. EpiSkin™, EpiDerm™, and SkinEthic™ are the most widely used for the assessment of skin irritation. According to OECD TG439, EpiSkin™ viability is judged to be noncorrosive when viability is above 50% after 15 min exposure and 42 h incubation. Thus, STEE is noncorrosive to human skin based on the *in vitro* assessment.

5. Conclusion

In this study, the purity of up to 43.4% for phenolic compounds in STEE was achieved by the use of response surface methodology and purification with SP700 macroporous

resin. STEE exhibits remarkable antioxidant activities against DPPH and hydroxyl radicals *in vitro*. Moreover, increasing the concentration of STEE leads to a reduction in intracellular ROS accumulation. Additionally, STEE supplementation enhances the levels of T-AOC, SOD, and GSH-Px, while reducing MDA content. Furthermore, STEE significantly downregulates the expression of inflammatory factors, including COX-2, iNOS, TNF-α, and IL-6, in L929 cells. Remarkably, STEE also exhibits inhibitory effects on collagenase and elastase, indicating its potential for safeguarding human skin from aging when employed in cosmetic or functional food applications.

Data Availability

The datasets used and/or analyzed during the current study are available from the corresponding authors on reasonable request.

Additional Points

Practical Application. *Sargassum thunbergii* has significant potential to protect the human skin from aging.

Conflicts of Interest

The authors declare that they have no conflicts of interest.

Authors' Contributions

Cui Lulu and Qu Haidong contributed equally to this work.

Acknowledgments

This work was supported by the Research Project of Province-Owned Public Scientific Research Institutes in Fujian Province (no. 2017R1003-13), a grant from the Marine Economy Innovation and Development Project of Fujian (16CZP010SF07), and a grant from Marine Economic Development Subsidy Program of Fujian (FJHJF-L-2019-3). We extend our special thanks to Yutian Pan (the Engineering Technological Center of Mushroom Industry, Minnan Normal University, China) for providing us with L929 cell line.

References

[1] D. R. Bickers and M. Athar, "Oxidative stress in the pathogenesis of skin disease," *Journal of Investigative Dermatology*, vol. 126, no. 12, pp. 2565–2575, 2006.

[2] R. M. Martinez, F. A. Pinho-Ribeiro, V. S. Steffen et al., "Topical formulation containing naringenin: efficacy against ultraviolet B irradiation-induced skin inflammation and oxidative stress in mice," *PLoS One*, vol. 11, no. 1, article e0146296, 2016.

[3] S. M. Bessada, R. Alves, and M. B. Oliveira, "Coffee silverskin: a review on potential cosmetic applications," *Cosmetics*, vol. 5, no. 1, pp. 5–15, 2018.

[4] S. J. Heo, S. C. Ko, S. M. Kang et al., "Inhibitory effect of diphlorethohydroxycarmalol on melanogenesis and its protective effect against UV-B radiation-induced cell damage," *Food and Chemical Toxicology*, vol. 48, no. 5, pp. 1355–1361, 2010.

[5] F. Ferreres, G. Lopes, A. Gil-Izquierdo et al., "Phlorotannin extracts from fucales characterized by HPLC-DAD-ESI-MSn: approaches to hyaluronidase inhibitory capacity and antioxidant properties," *Marine Drugs*, vol. 10, no. 12, pp. 2766–2781, 2012.

[6] M. J. Bae, F. Karadeniz, B. N. Ahn, and C. S. Kong, "Evaluation of effective MMP inhibitors from eight different brown algae in human fibrosarcoma HT1080 cells," *Preventive Nutrition and Food Science*, vol. 20, no. 3, pp. 153–161, 2015.

[7] N. J. Kang, D. H. Koo, G. J. Kang et al., "Dieckol, a component of Ecklonia cava, suppresses the production of mdc/ccl22 via down-regulating STAT1 pathway in interferon-γ stimulated HaCaT human keratinocytes," *Biomolecules & Therapeutics*, vol. 23, no. 3, pp. 238–244, 2015.

[8] T. S. Vo, S. K. Kim, B. Ryu et al., "The suppressive activity of Fucofuroeckol-A derived from brown algal Ecklonia stolonifera Okamura on UVB-induced mast cell degranulation," *Marine Drugs*, vol. 16, no. 1, p. 1, 2018.

[9] F. Erpel, R. Mateos, J. Perez-Jimenez, and J. R. Perez-Correa, "Phlorotannins: from isolation and structural characterization, to the evaluation of their antidiabetic and anticancer potential," *Food Research International*, vol. 137, article 109589, 2020.

[10] I. Generalic Mekinic, D. Skroza, V. Simat, I. Hamed, M. Cagalj, and Z. Popovic Perkovic, "Phenolic content of brown algae (Pheophyceae) species: extraction, identification, and quantification," *Biomolecules*, vol. 9, no. 6, p. 244, 2019.

[11] X. Zhou, M. Yi, L. Ding, S. He, and X. Yan, "Isolation and purification of a neuroprotective Phlorotannin from the marine algae Ecklonia maxima by size exclusion and high-speed counter-current chromatography," *Marine Drugs*, vol. 17, no. 4, p. 212, 2019.

[12] T. Wang, R. Jonsdottir, H. Liu et al., "Antioxidant capacities of phlorotannins extracted from the brown algae Fucus vesiculosus," *Journal of Agricultural and Food Chemistry*, vol. 60, no. 23, pp. 5874–5883, 2012.

[13] A. Leyton, J. R. Vergara-Salinas, J. R. Perez-Correa, and M. E. Lienqueo, "Purification of phlorotannins from Macrocystis pyrifera using macroporous resins," *Food Chemistry*, vol. 237, pp. 312–319, 2017.

[14] J. Kim, M. Yoon, H. Yang et al., "Enrichment and purification of marine polyphenol phlorotannins using macroporous adsorption resins," *Food Chemistry*, vol. 162, pp. 135–142, 2014.

[15] H. Li, Y. Liu, Y. Yi et al., "Purification of quercetin-3-O-sophoroside and isoquercitrin from Poacynum hendersonii leaves using macroporous resins followed by Sephadex LH-20 column chromatography," *Journal of Chromatography B*, vol. 1048, pp. 56–63, 2017.

[16] M. C. Kang, H. G. Lee, H. D. Choi, and Y. J. Jeon, "Antioxidant properties of a sulfated polysaccharide isolated from an enzymatic digest of *Sargassum thunbergii*," *International Journal of Biological Macromolecules*, vol. 132, pp. 142–149, 2019.

[17] J. A. Kim, C. S. Kong, and S. K. Kim, "Effect of *Sargassum thunbergii* on ROS mediated oxidative damage and identification of polyunsaturated fatty acid components," *Food and Chemical Toxicology*, vol. 48, no. 5, pp. 1243–1249, 2010.

[18] M. C. Kang, Y. Ding, E. A. Kim et al., "Indole derivatives isolated from brown alga *Sargassum thunbergii* inhibit adipogenesis through AMPK activation in 3T3-L1 preadipocytes," *Marine Drugs*, vol. 15, no. 4, pp. 119–128, 2017.

[19] K. Le Lann, S. Connan, and V. Stiger-Pouvreau, "Phenology, TPC and size-fractioning phenolics variability in temperate Sargassaceae (Phaeophyceae, Fucales) from Western Brittany: native versus introduced species," *Marine Environmental Research*, vol. 80, pp. 1–11, 2012.

[20] R. Ray, N. Agrawal, A. Sharma, and R. Hans, "Use of L-929 cell line for phototoxicity assessment," *Toxicology In Vitro*, vol. 22, no. 7, pp. 1775–1781, 2008.

[21] Z. Derakhshan, M. Ferrante, M. Tadi et al., "Antioxidant activity and total phenolic content of ethanolic extract of pomegranate peels, juice and seeds," *Food and Chemical Toxicology*, vol. 114, pp. 108–111, 2018.

[22] B. Chen, H. Chen, H. Qu et al., "Photoprotective effects of *Sargassum thunbergii* on ultraviolet B-induced mouse L929 fibroblasts and zebrafish," *BMC Complementary Medicine and Therapies*, vol. 22, no. 1, p. 144, 2022.

[23] B. Chen, L. Yu, J. Wu et al., "Effects of collagen hydrolysate from large hybrid sturgeon on mitigating ultraviolet B-induced photodamage," *Frontiers in Bioengineering and Biotechnology*, vol. 10, article 908033, 2022.

[24] K. J. Livak and T. D. Schmittgen, "Analysis of relative gene expression data using real-time quantitative PCR and the 2(-delta delta C(T)) Method," *Methods*, vol. 25, no. 4, pp. 402–408, 2001.

[25] J. S. Hwang, M. Y. Kwon, K. H. Kim et al., "Lipopolysaccharide (LPS)-stimulated iNOS induction is increased by glucosamine under normal glucose conditions but is inhibited by glucosamine under high glucose conditions in macrophage cells *," *The Journal of Biological Chemistry*, vol. 292, no. 5, pp. 1724–1736, 2017.

[26] D. Yu, H. Zhu, Y. Liu, J. Cao, and X. Zhang, "Regulation of proinflammatory cytokine expression in primary mouse astrocytes by coronavirus infection," *Journal of Virology*, vol. 83, no. 23, pp. 12204–12214, 2009.

[27] Z. Ren, J. Chen, and R. A. Khalil, "Zymography as a Research Tool in the Study of Matrix Metalloproteinase Inhibitors," *Methods in Molecular Biology*, vol. 1626, pp. 79–102, 2017.

[28] T. Shoko, V. Maharaj, D. Naidoo et al., "Anti-aging potential of extracts from Sclerocarya birrea (A. Rich.) Hochst and its chemical profiling by UPLC-Q-TOF-MS," *BMC Complementary and Alternative Medicine*, vol. 18, no. 1, pp. 1–14, 2018.

[29] Organisation for Economic Co-operation and Development, "Test no. 439," in *Vitro Skin Irritation*, Reconstructed Human Epidermis Test Method, 2019.

[30] K. Qiao, C. Fang, B. Chen et al., "Molecular characterization, purification, and antioxidant activity of recombinant superoxide dismutase from the Pacific abalone Haliotis discus hannai Ino," *World Journal of Microbiology & Biotechnology*, vol. 36, no. 8, p. 115, 2020.

[31] P. Rajneesh, J. Pathak, A. Chatterjee, S. P. Singh, and R. P. Sinha, "Detection of reactive oxygen species (ROS) in cyanobacteria using the oxidant-sensing probe 2',7'-dichlorodihydrofluorescein diacetate (DCFH-DA)," *Bio-Protocol*, vol. 7, no. 17, article e2545, 2017.

[32] D. H. Gam, J. H. Park, J. W. Hong, S. J. Jeon, J. H. Kim, and J. W. Kim, "Effects of Sargassum thunbergii extract on skin whitening and anti-wrinkling through inhibition of TRP-1 and MMPs," *Molecules*, vol. 26, no. 23, p. 7381, 2021.

[33] M. J. Yim, J. M. Lee, H. S. Kim et al., "Inhibitory effects of a Sargassum miyabei Yendo on Cutibacterium acnes-induced skin inflammation," *Nutrients*, vol. 12, no. 9, p. 2620, 2020.

[34] T. U. Jayawardena, S. Asanka, F. Shanura et al., "Sargassum horneri (Turner) C. Agardh ethanol extract inhibits the fine dust inflammation response via activating Nrf2/HO-1 signaling in RAW 264.7 cells," *BMC Complementary and Alternative Medicine*, vol. 18, no. 1, pp. 249–258, 2018.

[35] P. Otero, M. I. Lopez-Martinez, and M. R. Garcia-Risco, "Application of pressurized liquid extraction (PLE) to obtain bioactive fatty acids and phenols from Laminaria ochroleuca collected in Galicia (NW Spain)," *Journal of Pharmaceutical and Biomedical Analysis*, vol. 164, pp. 86–92, 2019.

[36] A. Abdelhamid, S. Lajili, M. A. Elkaibi et al., "Optimized extraction, preliminary characterization and evaluation of the in vitro anticancer activity of phlorotannin-rich fraction from the brown seaweed, Cystoseira sedoides," *Journal of Aquatic Food Product Technology*, vol. 28, no. 9, pp. 892–909, 2019.

[37] Y. Jin, K. Liu, J. Peng et al., "Rhizoma Dioscoreae Nipponicae polysaccharides protect HUVECs from H2O2-induced injury by regulating PPARgamma factor and the NADPH oxidase/ROS-NF-kappaB signal pathway," *Toxicology Letters*, vol. 232, no. 1, pp. 149–158, 2015.

[38] P. J. Park, S. J. Heo, E. J. Park et al., "Reactive oxygen scavenging effect of enzymatic extracts from Sargassum thunbergii," *Journal of Agricultural and Food Chemistry*, vol. 53, no. 17, pp. 6666–6672, 2005.

[39] J.-S. Park, J.-M. Han, D. Surendhiran, and B.-S. Chun, "Physicochemical and biofunctional properties of Sargassum thunbergii extracts obtained from subcritical water extraction and conventional solvent extraction," *The Journal of Supercritical Fluids*, vol. 182, p. 105535, 2022.

[40] A. R. Kim, T. S. Shin, M. S. Lee et al., "Isolation and identification of phlorotannins from Ecklonia stolonifera with antioxidant and anti-inflammatory properties," *Journal of Agricultural and Food Chemistry*, vol. 57, no. 9, pp. 3483–3489, 2009.

[41] D. H. Kuo, Y. S. Lai, C. Y. Lo, A. C. Cheng, H. Wu, and M. H. Pan, "Inhibitory effect of magnolol on TPA-induced skin inflammation and tumor promotion in mice," *Journal of Agricultural and Food Chemistry*, vol. 58, no. 9, pp. 5777–5783, 2010.

[42] S. Abbas, S. Alam, A. Pal, M. Kumar, D. Singh, and K. M. Ansari, "UVB exposure enhanced benzanthrone-induced inflammatory responses in SKH-1 mouse skin by activating the expression of COX-2 and iNOS through MAP kinases/NF-κB/AP-1 signalling pathways," *Food and Chemical Toxicology*, vol. 96, pp. 183–190, 2016.

[43] S. H. Eom, E. H. Lee, K. Park et al., "Eckol from Eisenia bicyclis inhibits inflammation through the Akt/NF-κB signaling in Propionibacterium acnes-induced human keratinocyte HaCat cells," *Journal of Food Biochemistry*, vol. 41, no. 2, article e12312, 2017.

[44] M. Dutot, R. Fagon, M. Hemon, and P. Rat, "Antioxidant, anti-inflammatory, and anti-senescence activities of a phlorotannin-rich natural extract from brown seaweed Ascophyllum nodosum," *Applied Biochemistry and Biotechnology*, vol. 167, no. 8, pp. 2234–2240, 2012.

[45] Y. Sugiura, M. Usui, H. Katsuzaki, K. Imai, and M. Miyata, "Anti-inflammatory effects of 6, 6'-bieckol and 6, 8'-bieckol from Eisenia arborea on mouse ear swelling," *Food Science and Technology Research*, vol. 23, no. 3, pp. 475–480, 2017.

[46] K. K. A. Sanjeewa, E. A. Kim, K. T. Son, and Y. J. Jeon, "Bioactive properties and potentials cosmeceutical applications of phlorotannins isolated from brown seaweeds: a review,"

Journal of Photochemistry and Photobiology. B: Biology, vol. 162, pp. 100–105, 2016.

[47] T. Quan, E. Little, H. Quan, Z. Qin, J. J. Voorhees, and G. J. Fisher, "Elevated matrix metalloproteinases and collagen fragmentation in photodamaged human skin: impact of altered extracellular matrix microenvironment on dermal fibroblast function," *Journal of Investigative Dermatology*, vol. 133, no. 5, pp. 1362–1366, 2013.

[48] N. Philips, S. Auler, R. Hugo, and S. Gonzalez, "Beneficial regulation of matrix metalloproteinases for skin health," *Enzyme Research*, vol. 2011, Article ID 427285, 4 pages, 2011.

[49] M. Toth, A. Sohail, and R. Fridman, "Assessment of gelatinases (MMP-2 and MMP-9) by gelatin zymography," *Methods in Molecular Biology*, vol. 878, pp. 121–135, 2012.

[50] M. M. Kim, Q. V. Ta, E. Mendis et al., "Phlorotannins in *Ecklonia cava* extract inhibit matrix metalloproteinase activity," *Life Sciences*, vol. 79, no. 15, pp. 1436–1443, 2006.

[51] M. J. Joe, S. N. Kim, H. Y. Choi et al., "The inhibitory effects of eckol and dieckol from Ecklonia stolonifera on the expression of matrix metalloproteinase-1 in human dermal fibroblasts," *Biological & Pharmaceutical Bulletin*, vol. 29, no. 8, pp. 1735–1739, 2006.

[52] C. Zhang, Y. Li, X. Shi, and S. K. Kim, "Inhibition of the expression on MMP-2, 9 and morphological changes via human fibrosarcoma cell line by 6,6'-bieckol from marine alga Ecklonia cava," *BMB Reports*, vol. 43, no. 1, pp. 62–68, 2010.

[53] M. Ou, X. Sun, J. Liang et al., "A polysaccharide from Sargassum thunbergii inhibits angiogenesis via downregulating MMP-2 activity and VEGF/HIF-1alpha signaling," *International Journal of Biological Macromolecules*, vol. 94, no. Part A, pp. 451–458, 2017.

[54] H. M. Chiang, T. J. Lin, C. Y. Chiu et al., "*Coffea arabica* extract and its constituents prevent photoaging by suppressing MMPs expression and MAP kinase pathway," *Food and Chemical Toxicology*, vol. 49, no. 1, pp. 309–318, 2011.

[55] D. Gingras, A. Renaud, N. Mousseau, E. Beaulieu, Z. Kachra, and R. Beliveau, "Matrix proteinase inhibition by AE-941, a multifunctional antiangiogenic compound," *Anticancer Research*, vol. 21, no. 1A, pp. 145–155, 2001.

[56] C. Zhang and S. K. Kim, "Matrix metalloproteinase inhibitors (MMPIs) from marine natural products: the current situation and future prospects," *Marine Drugs*, vol. 7, no. 2, pp. 71–84, 2009.

[57] I. K. Sundaram, D. D. Sarangi, V. Sundararajan, S. George, and S. S. Mohideen, "Poly herbal formulation with anti-elastase and anti-oxidant properties for skin anti-aging," *BMC Complementary and Alternative Medicine*, vol. 18, no. 1, p. 33, 2018.

[58] S. K. Jang, D. I. Lee, S. T. Kim et al., "The anti-aging properties of a human placental hydrolysate combined with dieckol isolated from Ecklonia cava," *BMC Complementary and Alternative Medicine*, vol. 15, no. 1, pp. 345–354, 2015.

[59] M. K. L. Riani, E. Anwar, and T. Nurhayati, "Antioxidant and anti-collagenase activity of Sargassum plagyophyllum extract as an anti-wrinkle cosmetic ingredient," *Pharmacognosy Journal*, vol. 10, no. 5, pp. 932–936, 2018.